from the most stable Pt_n cluster by addition of a single Pt atom to the unmodified compact Pt_n structure. This would imply the formation of an outgrowth which, except for the structure (8,21), cannot generate a structure with large spherical density. A significant reorganization is required to restore the compactness. In a similar way, the low-density surface of a crystal restructures relative to the crystal bulk. The number of MIDs is a good index number of the stability of the clusters of class A. Indeed, all its most stable clusters have the largest number of MIDs at the EHT level. This property is also true at the EHT-SO level except for the structures (11,1) and (12,1), which come after (11,2) and (12,2) while they have one MID less. These exceptions have been explained by the small geometrical constraints existing for bilayer clusters and by the sp populations.

When structures of class C are considered, the MID index number is only a helpful indication of the stability at the EHT level since some structures of class C have the largest cohesive energies without having the maximum number of MIDs. These structures have a large spherical density. Structures (8,24), (10,35), and (12,6) illustrate this point. As their SO contribution is weak, structures with the maximum number of MIDs ((8,21) from class C and (10,1) and (12,2) from class A) reappear as the most stable isomers at the EHT + SO level.

Since structures of class C are not suitable for an extension toward an infinite crystal and their cohesive energies are lower than for those of the fcc or hcp bulk, compounds of class A or B should prevail for the medium or large clusters. With such a growth, the mean number of MID per atom can converge to 6, the value for the bulk. For the small systems, the occurrence of some fragments of fcc or hcp type (Pt_3, Pt_4, Pt_5, Pt_6, Pt_{10}, Pt_{11}, Pt_{12}, and Pt_{13}) in the growth at the EHT + SO level is due more to their own compactness than to their classification as clusters of class A.

The EHT and EHT + SO methods are more selective than the simple Lennard-Jones interactions. For example, one Pt_{13} structure clearly emerges as the most stable within the EHT + SO framework while 987 structures are quasi-degenerate within a Lennard-Jones analysis.[3h]

The present results will be used to study the hydrogenation process of the Pt_n clusters.

Acknowledgment. This work has been supported by an ATP surface grant from the CNRS. We are pleased to thank Professor Fraissard for many discussions on the existence and the properties of small particles of platinum. We are grateful to Dr. Spanjaard for stimulating discussions on spin-orbit influence.

Registry No. Pt, 7440-06-4.

A Novel Isopiestic Measurement of Water Activity in Concentrated and Supersaturated Lithium Halide Solutions

C. B. Richardson* and C. A. Kurtz

Contribution from the Physics Department, University of Arkansas, Fayetteville, Arkansas 72701. *Received May 2, 1984*

Abstract: In a variation of the Stokes bithermal isopiestic method, single microscopic drops of lithium bromide and lithium iodide aqueous solution at room temperature are levitated electrodynamically in a closed chamber from which air is removed and to which is connected a vial of pure water at lower temperature. Water temperature is varied between −74 and +21 °C to measure concentrated and supersaturated solution water activity from 4.5×10^{-5} to 0.9. The results are compared with those of regular solution theory and the adsorption and stepped-hydration theories of Robinson and Stokes.

The isopiestic method for the determination of water activities in salt solutions is simple, precise, and general. Known amounts of nonvolatile solutes are placed in open containers in an isothermal enclosure into which water is introduced. At equilibrium the solution water activities are equal and the compositions are determined by weighing. With activities of reference solutions, e.g., NaCl, KCl, H_2SO_4, and $CaCl_2$, determined by vapor pressure and other measurements, the comparison method has yielded activities a_1 of hundreds of solutions over wide ranges of concentrations and temperatures.[1] With temperatures fixed to ±0.05 K or better, temperature differences between samples less than 10^{-4} K, and mass measurements precise to ±0.05%, the method yields composition ratios with a precision greater than 10^{-4} and ultimately, osmotic coefficients $\phi = -(N/\nu) \ln a_1$ with a precision greater than 10^{-3}. Here $N = [H_2O]/[X]$ is the solvent-solute and ν the ion-solute molar ratio.

A lower bound on a_1 is placed by the crystallization of the reference, e.g., $a_1 \geq 0.753$ for NaCl at 25 °C. In a variation on the method which avoids the lower bound, Stokes[2] replaced the solution reference with pure water at reduced temperature. He obtained good agreement with other measurements but did not push a_1 below 0.2889. A second lower bound is placed by crystallization of the unknown of course. Though many of the compounds listed in ref 1 have been measured to saturated solution, we know of no listings there for supersaturated solutions. Ionic solutions at the high concentrations of supersaturation may become ordered liquids for which water activity can serve as a probe.

We report here the results of an isopiestic study of lithium bromide and lithium iodide solutions by the Stokes method in which water activity is measured down to 4×10^{-5}. Our method differs in the handling of the sample. We have reduced its mass to 10^{-9} g, compared with the 1 g typical of isopiestic samples, have levitated it electrodynamically in a small sealed chamber from which air is removed, and have weighed it in situ and continuously with a noncontacting electrostatic balance.

With a microscopic spherical sample in a small chamber containing only water vapor, equilibrium is established much faster. More importantly, levitation of microscopic droplets allows supersaturation terminated only by homogeneous nucleation of crystallization.

We apply regular solution theory,[3] adsorption model theory,[4] and stepped-hydration model theory[5] to our results.

(1) Robinson, R. A.; Stokes, R. H., "Electrolyte Solutions"; Butterworths; London, 1959.
(2) Stokes, R. H. *J. Am. Chem. Soc.* **1947**, *69*, 1291.
(3) Pitzer, K. S. *Ber. Bunsenges. Phys. Chem.* **1981**, *85*, 952.
(4) Stokes, R. H.; Robinson, R. A. *J. Am. Chem. Soc.* **1948**, *70*, 1870.
(5) Stokes, R. H.; Robinson, R. A. *J. Soln. Chem.* **1973**, *2*, 173.

0002-7863/84/1506-6615$01.50/0

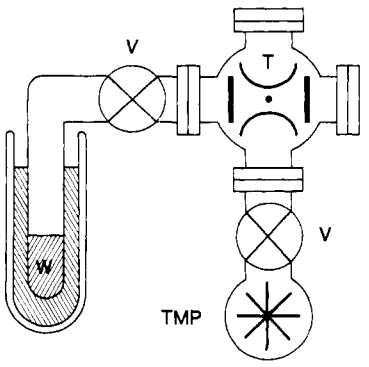

Figure 1. Schematic diagram of the isopiestic apparatus: T = ion trap, TMP = turbomolecular pump, V = valves, W = water.

Experimental Section

Materials. Lithium iodide and lithium bromide were obtained from Sigma Chemical Co. and Alfa Products, respectively. Each was recrystallized. The reference water was doubly distilled.

Method. A schematic diagram of the system is shown in Figure 1. The sample is levitated electrodynamically in an ion trap of design similar to that of Wuerker et al.[6] The trap is a quadrupole consisting of a powered ring electrode and two grounded end caps. We describe the operation briefly to explain its use as sample holder and mass balance.

With ideal geometry the ring has shape $z^2 - r^2/2 = -z_0^2$, the caps $z^2 - r^2/2 = z_0^2$ in cylindrical coordinates. If the ring potential is $V_0 \cos \Omega t$ and the caps are at zero potential, the electric field produced is proportional to the distance from trap center and the z motion of a particle of mass m, diameter d, carrying charge q is given by

$$m \frac{d^2z}{dt^2} = \frac{qz}{z_0^2} V_0 \cos \Omega t - 3\pi\eta d \frac{dz}{dt} \quad (1)$$

where we have used Stokes' law to include a viscous force. We will add the gravity force later. A similar equation describes the radial motion which we need not consider here. An approximate solution to eq 1 obtained following the example of Wuerker et al. illustrates the trapping action. In this $z \simeq Z + \delta$ where $\delta \ll Z$ is a micromotion at the frequency Ω and Z is the displacement over a cycle. With $d\delta/dt \gg dZ/dt$ we obtain after substitution

$$\delta = -\frac{qV_0Z(\cos \Omega t - b \sin \Omega t)}{mz_0^2\Omega^2(1 + b^2)} \quad (2)$$

$$\frac{d^2Z}{dt^2} = -\frac{q^2V_0^2Z}{2m^2z_0^4\Omega^2(1 + b^2)} - b\Omega \frac{dZ}{dt} \equiv -\frac{K}{m}Z - b\Omega \frac{dZ}{dt} \quad (3)$$

where $b = 3\pi\eta d/m\Omega$. Equation 3 is that of a damped harmonic oscillator. In air at atmospheric pressure $\eta = 1.8 \times 10^{-5}$ kg s^{-1} m^{-1}. With typical values $d = 10$ μm, $\rho = 2.6 \times 10^3$ kg m^{-3}, $\Omega = 1257$ s^{-1}, $q = 10^5$ e, $V_0 = 600$ V, $z_0 = 7$ mm, $b = 1$, $K = 4.5 \times 10^{-9}$ N m^{-1}, and $\omega = (K/m)^{1/2} = 58$ s^{-1}. The binding energy of the trapped particle is $E = Kz_0^2/2 = 6.9 \times 10^5$ eV, and its thermal motion amplitude $\bar{z} = (2kT/K)^{1/2} = 1.3$ μm at room temperature. Thus electrodynamic suspension yields a deep well with the particle essentially at rest at its center in the absence of gravity.

With gravity the equilibrium position is displaced $\Delta = mg/K$. This displacement may be nulled with a vertical electric field added to the quadrupole field of magnitude $V/\zeta = mg/q$ where $\zeta \simeq z_0$ and $2V$ is the potential difference between the caps. Thus the trap may be used as a balance to measure relative mass.[7]

The trap cylinder is made of stainless steel, the end caps of nickel mesh, and the insulating spacers of Macor ceramic. It is supported on a stainless-steel post and placed in the center of a stainless-steel 6-way cross. Ports are connected to the reference water vial through an Ace Glass bakeable stopcock and to a Balzers 170 L s^{-1} turbomolecular pump through a Varian precision leak valve. Three ports are sealed with Pyrex windows for illumination of the particle by light from a Spectra Physics 5-mW helium–neon laser and visual and phototube detection.

The sealed chamber has a volume of about 400 cm^3. It and the trap are easily disassembled and are cleaned frequently. When reassembled the system is evacuated and baked at 200 °C for several hours. A base pressure of 10^{-8} torr is achieved.

After evacuation the chamber is filled with room air which is passed through a particulate filter and liquid-nitrogen-cooled vapor trap. Doubly distlled water is placed in the water vial, which is then pumped for about 1 min and sealed. The free water surface has an area of about 3 cm^2. It is roughly 30 cm from the trap center. The salt solution is loaded into a stainless-steel gun of special design having an orifice 10 μm in diameter. Roughly 3 mm below this orifice is a ring to which a voltage is applied to charge the conducting droplets. The flange-mounted gun is placed about 40 mm above the trap center. A pressure pulse of about 10^{-3}-s duration is applied to the gun injecting 1 to 5 particles. All but one are driven out by manipulating trap power. The gun is then removed, its port sealed, and the chamber quickly evacuated to a pressure of 10^{-6} torr and sealed. During the evacuation the particle crystallizes and becomes anhydrous.

A cooling bath surrounds the water vial. Its temperature is measured to ±0.05 K with a type K thermocouple and a digital voltmeter. Temperatures as low as 200 K are obtained. The temperature of the levitated particle is assumed to be equal to that of the chamber which is measured by a thermometer to ±0.05 K.

The results from a portion of a measurement cycle for a lithium bromide particle are shown in Figure 2. Particle temperature was 23.40 ± 0.05 K over the period. Measurement precision and the establishment of equilibrium are illustrated in the balance voltage vs. thermocouple emf plot of Figure 3. In the worst case a data point deviates in solution composition $\Delta N/N = 0.003$ or in water temperature $\Delta T = 0.1$ K from the smooth curve through the set. Here $N = [H_2O]/[LiBr]$. Apparent in this plot is that portion of the cycle during which the water source was supercooled.

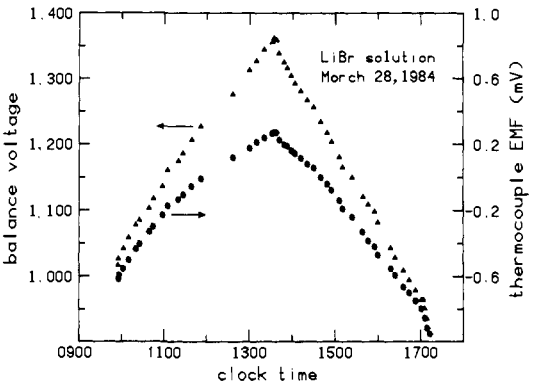

Figure 2. Data for lithium bromide droplet at 23.4 °C. Balance voltage gives composition, thermocouple emf vapor pressure.

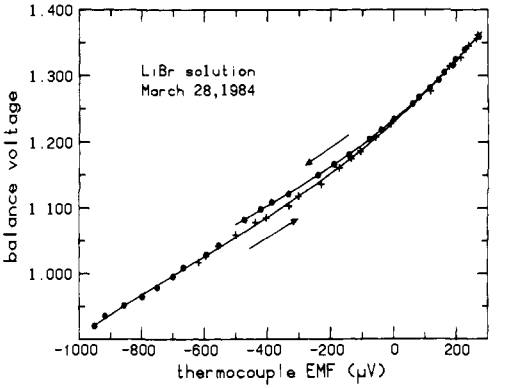

Figure 3. Figure 2 data showing reproducibility of results. Note approximate 15 °C supercooling of water.

Table I. Saturated Solution at 23 °C

compd	composition $[H_2O]/[LiX]$	osmotic coefficient ϕ
LiBr	2.75 ± 0.01	4.12 ± 0.03
LiI	4.54 ± 0.02	3.88 ± 0.04

Results

We summarize in Figures 4 and 5 our measurements of the water activities at $T = 23$ °C of concentrated and supersaturated solutions of lithium bromide and lithium iodide. Here are plotted

(6) Wuerker, R. F.; Shelton, H.; Langmuir, R. V. *J. Appl. Phys.* **1959**, *30*, 342.

(7) Davis, E. J.; Ray, A. K. *J. Colloid Interface Sci.* **1980**, *75*, 566.

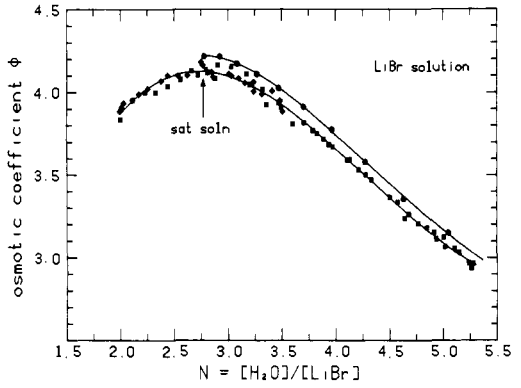

Figure 4. Osmotic coefficient of lithium bromide solution at 23 °C. Data from ref 1 shown as solid circles.

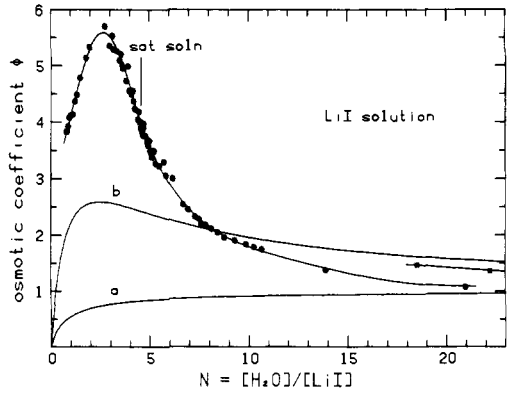

Figure 5. Osmotic coefficient of lithium iodide solution. Data from ref 1 shown as solid squares. Curve a: ideal solutions. Curve b: regular solution with $w = -7.5$, $b = 1$.

the osmotic coefficients $\phi = -(N/2) \ln a_1$ vs. N. The curves which best fit the data are given by equations in the Appendix. Arrows indicate saturated solutions, the results for which are shown in Table I. For comparison we have also plotted results from ref 1. Solution theory curves which are discussed below are included in Figure 5.

Discussion

The lithium halide solutions with supersaturation span the composition spectrum from nearly pure water to nearly pure salt. Ion–ion interaction is dominant in the concentrated solution in which near-crystalline order is expected. The water dipole is effective in determining this order, however, as is apparent from the five crystalline phases, four hydrated, of lithium iodide at room temperature.[8] At intermediate concentration, ion–dipole interactions should be dominant.

The ion–ion, ion–water, and water–water interactions are the principal determinants of the non-ideality parameter w of regular solution theory[9] as applied to electrolytes by Pitzer[3]

$$\ln a_1 = \ln x_1 + w z_2^2 \tag{4}$$

Here a_1 is the water activity, $x_1 = n_1/(n_1 + \nu n_2)$ is the water mole fraction where n_1 and νn_2 are the moles of water and salt ions, respectively, and $z_2 = \nu n_2/(b n_1 + \nu n_2)$. The constant b is related to molar volumes. We rewrite eq 4 in terms of the osmotic coefficient ϕ and the molar ratio $N = n_1/n_2$ as

$$\phi = (N/2) \ln [(N + 2)/N] - 2wN/(bN + 2)^2 \tag{5}$$

Pitzer[3] has shown that excellent agreement between theory and experiment for ionic solutions over the entire range of x_1 can be obtained with constant w and b.

We have attempted to fit eq 5 to our lithium iodide results, without success. For example, the curve for $w = -7.5$, $b = 1$ is shown. For reference, the ideal solution ($w = 0$) curve is also plotted. We conclude from these examples that regular solution theory is applicable to ionic solutions only if their behavior does not depart too much from that of an ideal solution.

Stokes and Robinson[4] measured the water activity of supersaturated calcium nitrate solution and concluded, "These phenomena suggested the possibility that at high ion concentrations the system could be treated as an adsorbent (calcium nitrate)–adsorbate (water)". To analyze the results they applied with success the theory of Brunauer, Emmet, and Teller[10] developed for adsorption on solids. Other solutions thus analyzed include LiCl and LiBr. We have applied BET to our results.

For solutions BET is

$$\frac{a}{(1 - a)N} = \frac{1}{cs} + \frac{(c - 1)a}{cs} \tag{6}$$

where a is water activity, N is again the number of water molecules per adsorbent molecule, s is the number of adsorption sites per molecule, and $\ln c = (Q_a - Q_l)/kT$ where Q_a is the water molecule binding energy in the first layer and Q_l that in the second and higher layers. With this perspective we show in Figure 6 the "adsorption isotherm", N vs. a for lithium iodide. This is a type II isotherm in Brunauer's classification scheme.[11] The knee

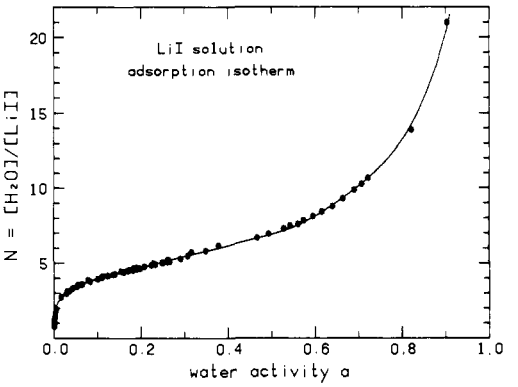

Figure 6. Adsorption isotherm of LiI at 23 °C.

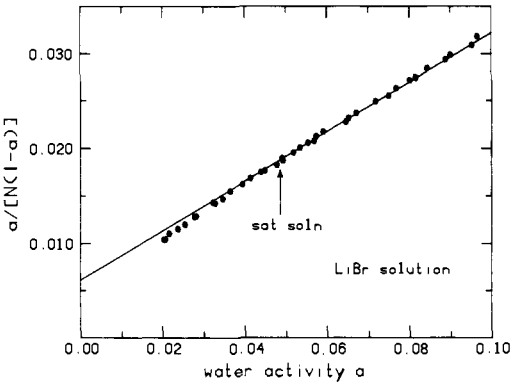

Figure 7. BET theory applied to lithium bromide solution. Result $Q_a = Q_l + 3.78kT$; $s = 3.73$. Note departure at high concentration.

Table II. Hydration of Lithium Halides in Concentrated Solutions

compd	adsorption energy Q_a,[a] eV	adsorption sites s	N range[b]
LiCl[c]	0.529	3.64	1.9–4.6
LiBr	0.552 (0.552)[c]	3.73 (3.82)[c]	2.5–5.0
LiI	0.576	3.94	2.9–6.0

[a] We have set $Q_l = 0.456$ eV, the heat of vaporization of bulk water at 23 °C. [b] $N = [H_2O]/[LiX]$. [c] Reference 4.

(8) Kurtz, C. A.; Richardson, C. B. *Chem. Phys. Lett.* **1984**, *109*, 190.
(9) van Laar, J. J. *Z. Phys. Chem.* **1919**, *72*, 723.
(10) Brunauer, S.; Emmett, P. H.; Teller, E. *J. Am. Chem. Soc.* **1938**, *60*, 309.
(11) See: Adamson, A. W. "Physical Chemistry of Surfaces"; John Wiley and Sons: New York, 1982.

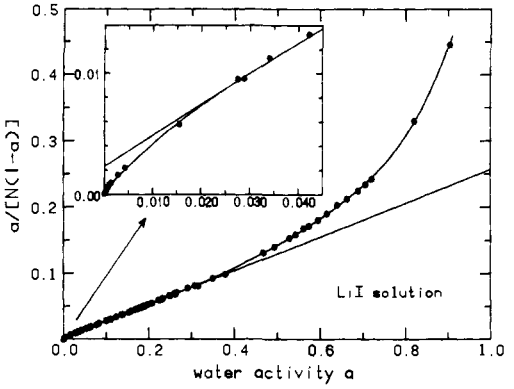

Figure 8. BET theory applied to lithium iodide solution. Result $Q_a = Q_l + 4.71kT$; $s = 3.94$.

around $N = 3$ is evidence of the completion of the monolayer.

In Figure 7 we show a plot of measured $a/[(1 - a)N]$ vs. a and the best-fitting linear curve for $0.05 \leq a \leq 0.32$ for lithium bromide. We find $\ln c = 3.78$ and $s = 3.73$. It is apparent that the BET model predicts too little adsorption for $a \leq 0.05$. In Figure 8 we show the same for lithium iodide using data for $0.03 \leq a \leq 0.38$ to obtain $\ln c = 4.71$ and $s = 3.94$. Again the model predicts too little adsorption at low pressure. At high pressure it predicts too much. It is noteworthy that for a variety of adsorbates on bulk adsorbents BET departs from experiment at high and low pressures as it does here. We summarize in Table II the results of this analysis for the lithium halides.

The trend to larger Q_a and s with an increase in anion size observed by Robinson and Stokes[4] is further demonstrated here. Stokes and Robinson[5] have argued that the adsorption is primarily on the lithium and is less opposed by larger anions. The failure of the model at small N is as expected. As the solutions take on the order of molten and crystalline salts, the water molecules leave the lithium ions to enter the "cells" forming. For lithium iodide the model breaks down with increasing N before the second layer is complete, predicting too little vapor pressure. Similar breakdown is observed for adsorption on bulk solids, for example nitrogen on powdered potassium chloride.[11]

Alternative adsorption theories[11] could be used in analysis. But BET is adequate to support further Stokes' and Robinson's 1948 idea that over a range of solution concentrations for which the water–ion interaction should be dominant, the interaction is much like that in two dimensions on a bulk surface.

Stokes and Robinson[5] have also presented a theory of stepwise hydration of ions in aqueous electrolytes to account for water activity. Excellent agreement with experiment is obtained for several solutions including LiCl and LiBr to 20 mol·kg^{-1} concentration. Stokes and Robinson applied their theory as follows. The anion was assumed unhydrated and a maximum number of hydration sites on the cation was chosen (5 for Li^+). A measured water activity value was used to calculate with volume fraction statistics the average hydration number h at that concentration. The free energy change ΔG_n with attachment of the nth water molecule was then chosen to yield the same value of h. To simplify the procedure, Stokes and Robinson limited the choice to $\Delta G_n = \Delta G - (n - 1)\delta G$, where ΔG and δG are constant. With the same ΔG_n and another activity–concentration value the hydration numbers are again calculated and compared. This is repeated for the entire data set until the values of ΔG and δG are found

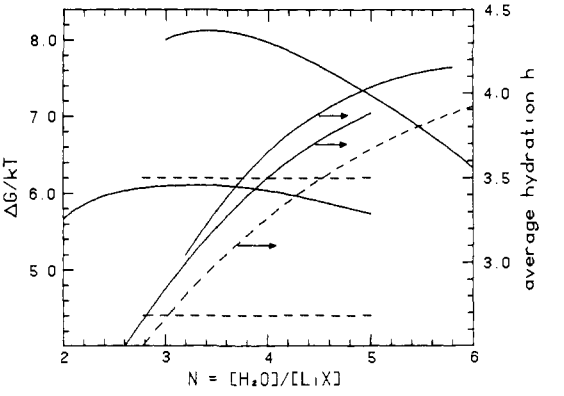

Figure 9. Lithium ion hydration energy and number: upper, LiI; center, LiBr; lower, LiCl; dashed curves, ref 5.

which minimize the difference between theory and experiment. We show in Figure 9 the hydration number h for LiCl and the $\Delta G/kT$ for LiCl and LiBr obtained. (For both $\delta G \simeq \Delta G/5$.)

We have applied the theory to our measurements. Following Stokes and Robinsin we set the number of lithium sites at 5 but make $\delta G = \Delta G/5$. Rather than searching for a constant ΔG, however, we vary it as required to give exact agreement between theoretical and experimental values of water activity. The results for hydration number and $\Delta G/kT$ are shown in Figure 9. Especially noteworthy is the decrease in ΔG with increasing water content. We speculate that this decrease may be due both to an increasing water–water interaction and a decreasing water–ion interaction.

Finally, Pitzer[12] has reviewed advances in electrolyte theory since Debye and Huckel. Pitzer and Mayorga[13] have applied a semiempirical equation to fit osmotic coefficient data for 227 pure aqueous electrolytes at concentrations up to 6 mol·kg^{-1}. Richardson and Spann[14] have shown, using their results for supersaturated ammonium sulfate, that the equation is applicable to about 30 mol·kg^{-1}. Because the parameters in this equation are not as simply identified with physical quantities as those in the regular solution, adsorption, and hydration theories we have not applied it here.

Acknowledgment. J. F. Spann assisted in the laboratory and participated in many helpful discussions. This work was supported by a grant from the National Science Foundation, ATM 8202766.

Appendix

The curve which best fits the lithium bromide results shown in Figure 4 is given by the equation $\phi = -0.58626 + 4.08603N - 1.0989N^2 + 0.085693N^3$, for $2.0 \leq N \leq 5.3$ with a standard deviation 0.03. The curve which best fits the lithium iodide results shown in Figure 5 is given by the equation $\phi = 2.9901 + 0.46218N + 1.0578N^2 - 0.43839N^3 + 0.042619N^4$, for $0.65 \leq N \leq 4.5$. For $4.5 \leq N \leq 18$ $\phi = 13.892 - 3.9386N + 0.52457N^2 - 0.035454N^3 + (1.1821 \times 10^{-3}N^4) - (1.5423 \times 10^{-5}N^5)$. The standard deviation for each is 0.01.

Registry No. H_2O, 7732-18-5; LiBr, 7550-35-8; LiI, 10377-51-2.

(12) Pitzer, K. S. *Acc. Chem. Res.* **1977**, *10*, 371.
(13) Pitzer, K. S.; Mayorga, G. *J. Phys. Chem.* **1973**, *77*, 2300.
(14) Richardson, C. B.; Spann, J. F. *J. Aerosol Sci.* **1984**, *15*, 563.